First-principles-based $s^{\pm}$-wave modeling for iron-based superconductors: Specific heat and nuclear magnetic relaxation rate

N. Nakai,[1,2,*] H. Nakamura,[1,2,3] Y. Ota,[1,2] Y. Nagai,[1,2,3] N. Hayashi,[2,4] and M. Machida[1,2,3]
[1]*CCSE, Japan Atomic Energy Agency, 6-9-3 Higashi-Ueno, Taito-ku, Tokyo 110-0015, Japan*
[2]*CREST, JST, 4-1-8 Honcho, Kawaguchi, Saitama 332-0012, Japan*
[3]*TRIP, JST, 5 Sanban-cho, Chiyoda-ku, Tokyo 110-0075, Japan*
[4]*N2RC, Osaka Prefecture University, 1-2 Gakuen-cho, Naka-ku, Sakai 599-8570, Japan*
(Received 28 July 2010; published 2 September 2010)

In order to consistently explain controversial experimental results on superconducting states observed by different probes in typical iron-based superconductors, we construct a realistic multiband $s^{\pm}$-wave pairing model by combining the quasiclassical formalism with the first-principles calculation. The model successfully resolves the controversies in contrast to the fact that simplified models such as two-band $s^{\pm}$-wave one fail to do. A key in the model is the existence of relatively small gaps which leads to material-dependent peculiarities.

DOI: 10.1103/PhysRevB.82.094501 PACS number(s): 74.20.−z, 74.25.Jb, 74.70.Dd

I. INTRODUCTION

The discovery of the iron-pnictide superconductor $LaFeAs(O_{1-x}F_x)$ (Ref. 1) made a striking impact on materials science, because this compound includes the element of the most familiar ferromagnetic metal, Fe, as a main component. The transition temperature T_c in the so-called "1111" compounds RFeAs$(O_{1-x}F_x)$ (R=Pr, Nd, and Sm) exceeds 50 K, which is the highest except for high-T_c cuprates. In addition to the high transition temperature, the variety of related materials is quite rich. For example, "122" compounds $(A_{1-x}B_x)Fe_2As_2$ (A=Ba, Sr, and Ca, B=K, Cs, and Na) and "11" compounds $Fe(Se_xTe_{1-x})$ are the typical family materials, whose element substitutions are widely possible.[2] In particular, the superconductivity is surprisingly robust against substitutions of Ni and Co for Fe.

In contrast to the discovery rush of family compounds, their superconducting states still remain elusive. There is no established pairing-symmetry model explaining all experimental results consistently. In the early days, puzzling experimental data were reported. In spite of sharp resistivity drops and clear Meissner signals at the superconducting transition T_c, the jump of C/T, where C is the specific heat and T is the temperature, was hardly observable in 1111 compounds. The reason was initially ascribed to a large phonon contribution which masks an electronic one. Afterwards, a tiny but clear jump at T_c and the concave-down temperature-dependent C/T below T_c were confirmed in not only 1111 compounds[3,4] but also structurally equivalent $LaFeP(O_{1-x}F_x)$.[5,6] These features are characteristic of a typical multigap superconductor, in which rather small superconducting gap coexists with large main gaps.[7,8] In this paper, we clarify that such a multigap structure consistently explains all experimental observations of 1111 compounds by means of a realistic five-band $s^{\pm}$-wave gap model based on a first-principles calculation. A striking result of the model is a natural reproduction of the nuclear magnetic relaxation rate $1/T_1$ below T_c.

On the other hand, 122 compounds experimentally exhibit large jumps and exponential behavior in C/T like conventional superconductors.[4,9–11] Moreover, the power law in the T dependence of $1/T_1$ below T_c is different from that of 1111 compounds.[2,12–15] In fact, an angle-resolved photoemission spectroscopy (ARPES) study reported that all gaps fully open and the difference between their gap amplitudes is not so significant.[16] In this case, we reveal that the multigap structure according to ARPES data can consistently explain the specific heat and $1/T_1$ data without any assumptions except for $s^{\pm}$-wave paring symmetry.[17,18] From the present analyses on 1111 and 122 compounds, it is found that the existence of the relatively small gap gives rise to the material variety. We believe that this fact has a key role on the quest for the high-temperature superconducting mechanism. In this paper, in order to confirm the multigap idea, we examine low-lying excitations in their superconducting states through C/T and $1/T_1$.

II. MODELING AND CALCULATION METHOD

Let us present a procedure to construct the realistic multiband-gap model. For the band structure around the Fermi level E_F, we perform first-principles calculations,[19] which provide multiple Fermi surfaces and their density of states (DOS) at E_F. In the evaluation of superconducting gaps for multiband superconductors, we select key data among all experimental ones. For example, ARPES measurements are so successful for 122 compounds[16] that the gap amplitudes on each band are available in the 122 cases. On the other hand, ARPES data for 1111 compounds[20,21] are not so clear as 122 ones. Therefore, we instead utilize data of the specific heat[5] and the penetration depth[22,23] in 1111 cases to estimate the gap amplitudes. Those data clearly suggest that the pairing symmetry is full gap but a small single or small multigaps coexist with main large gaps.[22–27]

Here, we write down on the expression for C/T using the quasiclassical treatment on multiband systems due to lack of explicit literatures, while we can refer Refs. 28–30 for $1/T_1$ in the multiband quasiclassical treatment. The T dependence of C/T is calculated by the second derivative of the free energy. The free energy can be evaluated by the quasiclassical theory of superconductivity,[31,32] which is a mean field but convenient treatment in evaluating superconducting proper-

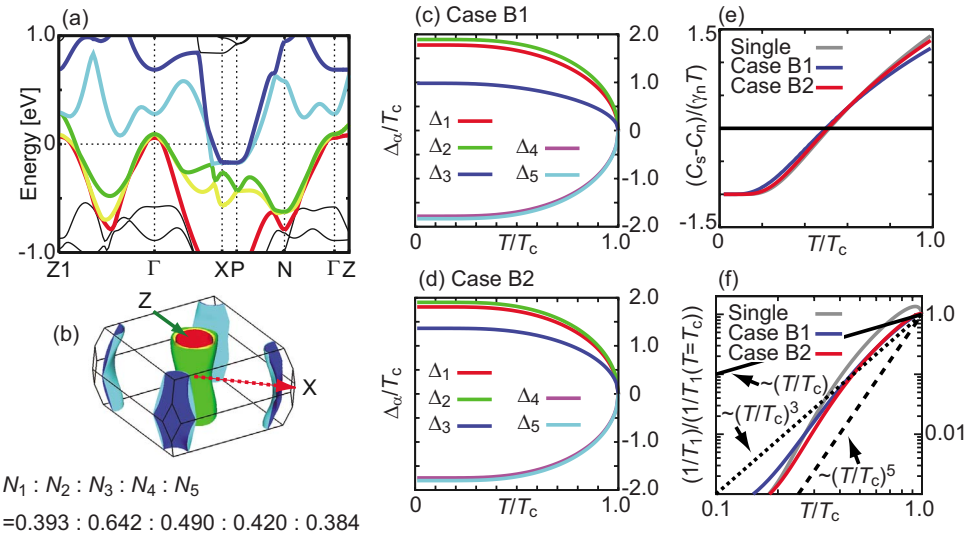

FIG. 1. (Color online) (a) The band structure calculated by the generalized gradient approximation using structural measurement values of $BaFe_2As_2$. (b) The Fermi surfaces and the density of states at the Fermi energy. Indices (α=1, 2, 3, 4, and 5) are assigned from Γ (zone center) to X. Temperature dependences of the superconducting pair-potential Δ_α are displayed in (c) and (d). Here, "B" of case B1 or B2 stands for $BaFe_2As_2$. (e) Temperature dependences of $(C_s-C_n)/T$. $C_{s(n)}$ is the specific heat of the superconducting state (normal state). (f) Temperature dependences of the nuclear magnetic relaxation rate $1/T_1$.

ties. To calculate C/T and $1/T_1$, we need the T dependence of the multiple superconducting pair-potential Δ_α on each band. For this purpose, we solve the gap equations for multiband superconductors.[33] With Matsubara frequency $\omega_n=(2n+1)\pi T$, the gap equation is written as

$$\Delta_\alpha = 2\pi T \sum_{\omega_n>0} \sum_\beta \lambda_{\alpha\beta} f_\beta(i\omega_n), \tag{1}$$

$$\Delta_\alpha^* = 2\pi T \sum_{\omega_n>0} \sum_\beta \lambda_{\alpha\beta} f_\beta^\dagger(i\omega_n), \tag{2}$$

where α and β stand for the band index and $\lambda_{\alpha\beta}$ is the effective coupling constant. In addition, $\lambda_{\alpha\beta}=N_\beta\lambda_{\beta\alpha}/N_\alpha$ with N_α being DOS at E_F for α band. $\lambda_{\alpha\alpha}$ comes from the intraband interaction and $\lambda_{\alpha\beta}$, where $\alpha\neq\beta$, gives the pair hopping between the different bands. The effective coupling constants $\lambda_{\alpha\beta}$'s are given as parameters to reproduce the experimental results for the superconducting gaps.

The quasiclassical Green's functions $g_\alpha(i\omega_n)$, $f_\alpha(i\omega_n)$, and $f_\alpha^\dagger(i\omega_n)$ follow the Eilenberger equations as:

$$\omega_n f_\alpha(i\omega_n) = \Delta_\alpha g_\alpha(i\omega_n), \tag{3}$$

$$\omega_n f_\alpha^\dagger(i\omega_n) = \Delta_\alpha^* g_\alpha(i\omega_n), \tag{4}$$

$$g_\alpha^2(i\omega_n) = 1 - f_\alpha(i\omega_n) f_\alpha^\dagger(i\omega_n), \tag{5}$$

where Re $g_\alpha(i\omega_n)>0$ for $\omega_n>0$. The free-energy difference between the superconducting and normal states,[31,32,34,35] $F_{sn}=F_{\text{super}}-F_{\text{normal}}$, is expressed as

$$F_{sn} = -2\pi T \sum_\alpha \sum_{\omega_n>0} N_\alpha \left[\frac{1-g_\alpha(i\omega_n)}{1+g_\alpha(i\omega_n)} \Delta_\alpha f_\alpha^\dagger(i\omega_n) \right], \tag{6}$$

which demands the solutions of Eqs. (1)–(5),

$$f_\alpha(i\omega_n) = \frac{\Delta_\alpha}{\sqrt{\omega_n^2+|\Delta_\alpha|^2}}, \tag{7}$$

$$f_\alpha^\dagger(i\omega_n) = \frac{\Delta_\alpha^*}{\sqrt{\omega_n^2+|\Delta_\alpha|^2}}, \tag{8}$$

$$g_\alpha(i\omega_n) = \frac{\omega_n}{\sqrt{\omega_n^2+|\Delta_\alpha|^2}}. \tag{9}$$

The cut-off frequency ω_c is introduced as $\Sigma_{\omega_n>0}^{\omega_c}$ in Eqs. (1), (2), and (6).[36] Equation (6) indicates that F_{sn} can be directly evaluated by DOS N_α obtained from first-principles calculations and the gap values Δ_α.

Since C/T at constant volume is generally obtained by $C/T=\partial S/\partial T=-\partial^2 F/\partial T^2$, the specific heat in the superconducting state is expressed as

$$\frac{C_s-C_n}{T} = -\frac{\partial^2 F_{sn}}{\partial T^2}, \tag{10}$$

where $C_{s(n)}$ is the specific heat of the superconducting state (normal state) and C_n/T is given by the Sommerfeld coefficient, γ_n. Then, we numerically calculate $\partial^2 F_{sn}/\partial T^2$ to obtain C_s/T. As for $1/T_1$,[28–30] we also use N_α and Δ_α obtained in the same framework.

III. CALCULATION RESULTS

A. 122 superconducting compounds

Let us present the calculation results. The first focus is 122 compounds. Figure 1(a) shows the band structure of $BaFe_2As_2$. This result is obtained by using the generalized gradient approximation (GGA) based on the measured struc-

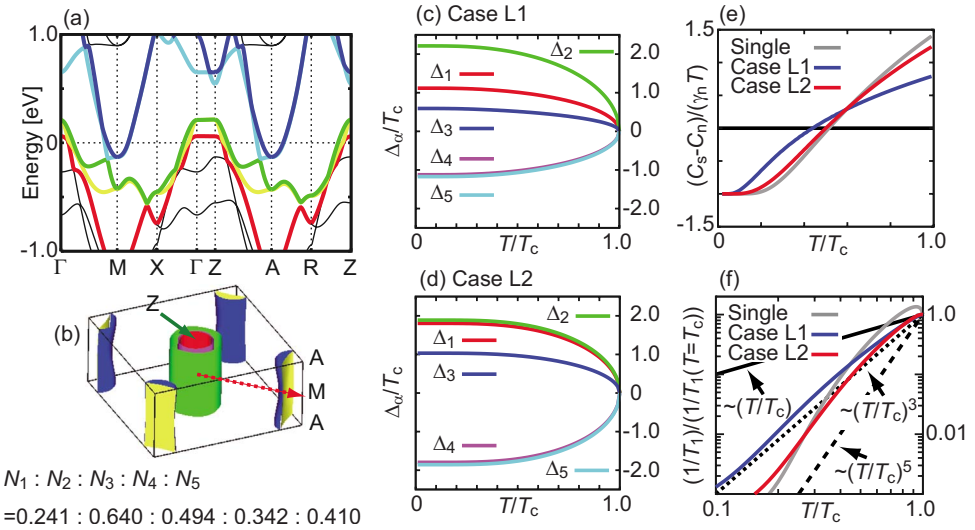

FIG. 2. (Color online) (a) The band structure calculated by the generalized gradient approximation using structural measurement values of LaFeAsO. (b) The Fermi surfaces and the density of states at the Fermi energy. Indices (α=1, 2, 3, 4, and 5) are assigned from Γ (zone center) to M. Temperature dependence of the superconducting pair-potential Δ_α in (c) and (d). Here, "L" of case L1 or L2 stands for LaFeAsO. (e) Temperature dependences of $(C_s-C_n)/T$. $C_{s(n)}$ is the specific heat of the superconducting state (normal state). (f) Temperature dependences of the nuclear magnetic relaxation rate $1/T_1$.

tural data.[37] The obtained Fermi surfaces are displayed in Fig. 1(b). The calculation gives DOSs at E_F, which are input parameters in the gap Eqs. (1) and (2) and the free energy Eq. (6). Each DOS at E_F is written as N_α, where α is numbered as α=1, 2, 3, 4, and 5 from Γ point (zone center) to X as shown in Fig. 1(b) and α=1–3 (4–5) correspond to hole (electron) bands. Throughout this paper, we adopt $s^{\pm}$-wave pairing model since other choices fail to reproduce the experimental data consistently. The positive (negative) sign is assigned to Δ_α of hole (electron) bands (Δ_α are assumed to be real). The calculated T dependence of Δ_α just follows the ARPES result[16] (case B1) as shown in Fig. 1(c). On the other hand, in Fig. 1(d) we prepare, for comparison, another data set (case B2) with the minimum $|\Delta_3|$ being slightly bigger than the ARPES result. Figure 1(e) shows the T dependences of C/T. Both cases B1 and B2 show no significant difference from the weak-coupling single-band Bardeen-Cooper-Schrieffer (BCS) result. One of the reasons is that the weighting of the small-gap band is small compared to total one, i.e., the ratio N_3/N_t is 0.2, where N_t is the total DOS ($N_t=\Sigma_\alpha N_\alpha$). Moreover, the gap-amplitude difference between the minimum $|\Delta_3|$ and the maximum $|\Delta_2|$ is not so large, where $|\Delta_3|/|\Delta_2|\sim 0.5(\sim 0.7)$ for case B1 (B2). Moreover, $|\Delta_2|/T_c\sim 2$, which is bigger than the single-band's value 1.76, just enhances C/T at T_c slightly. As a result, the difference in C/T is not large among cases B1, B2, and single-band BCS case. The T dependences of C/T in cases B1 and B2 are consistent with the experimental observations.[4]

On T dependence of $1/T_1$, both the cases show significant differences from the single-band BCS case as shown in Fig. 1(f). The coherence peak just below T_c is absent in both cases B1 and B2, because the cancellation between "+" and "–" signs of Δ_α is effective. In contrast, in the single-band BCS case, even if the damping rate of the quasiparticle is taken large as $\eta=0.1T_c$, the peak is clearly observable as seen in Fig. 1(f). Moreover, the low-lying excitation arising from the small gap $|\Delta_3|$ alters T dependence of $1/T_1$ compared to the single-band BCS case. We point out that the five-band model case B1 successfully reproduces the experimental results of C/T and $1/T_1$.[4,14]

B. 1111 superconducting compounds

We next turn to 1111 compounds. At first, based on GGA with measured structural parameters,[38] we obtain the band structure of LaFeAsO as shown in Fig. 2(a). The band index is also numbered as α=1, 2, 3, 4, and 5 from Γ (zone center) to M. The five Fermi surfaces are displayed in Fig. 2(b), where N_1, N_2, and $N_3(N_4,N_5)$ are the DOS at E_F of hole (electron) bands. We prepare two types of multigap structures, cases L1 and L2, whose T dependences of Δ_α are plotted in Figs. 2(c) and 2(d), respectively. Case L1 considers a medium gap between the maximum and minimum gaps based on the experimental data of the specific heat[3–5] and the penetration depth,[23] while case L2 gives four large gaps and one small gap as case B1 in Fig. 1(c) according to recent NMR experiments on slightly higher T_c materials.[13,39,40]

Figure 2(e) shows T dependence of C/T for both cases L1 and L2. When the amplitude difference between the minimum and maximum gaps becomes large, the jump of C/T at T_c decreases. In addition, case L1 reproduces the concave-down behavior as observed in $LaFeP(O_{1-x}F_x)$.[5] Thus, the small-jump feature and the concave-down behavior in C/T suggest not only the existence of a small gap but also that of a medium-gap band, whose contributions are significant compared to 122 compounds. We then expect that case L1 is the most realistic candidate in reproducing the most of experiments. On the other hand, we mention that a slightly higher T_c case shows a large jump,[39] which is consistent with C/T of case L2 in Fig. 2(e). The reason is identical to that as explained in case B1.

Figure 2(f) shows T dependence of $1/T_1$ for both cases L1 and L2. We find that case L1 surprisingly exhibits T^3 behavior of $1/T_1$ up to experimentally accessible low T. The low-lying excitations due to the small gap push the exponential behavior of $1/T_1$ into a further lower temperature region. Moreover, the peak just below T_c does not appear because of the cancellation due to $\pm$ signs.[30] The most of 1111 compounds show T^3 dependence in $1/T_1$ below T_c,[2,14] which suggests that case L1 is the best as noted in Fig. 2(f). On the other hand, in slightly higher T_c 1111 materials,[13,39] T dependence of $1/T_1$ shows T^5 as case L2 in Fig. 2(f), which are principally equivalent to that for case B1 in Fig. 1(f). Furthermore, As-deficient 1111 compounds showing a slightly higher T_c also exhibit T^5 behavior as very recently reported in Ref. 40. Although these results might be relevant to impurity effects, the essence can be understood by the story described above.

IV. DISCUSSION

Here, let us discuss the other important experimental data, i.e., superfluid density. In addition to C/T and $1/T_1$, we investigate the T dependences of the superfluid density, which are not shown here. On this measurement, the present model and earlier two-band models show almost both equivalent results consistent with experiments. This is because the number of gaps is not crucial, but only the existence of a small gap is just of importance in contrast to C/T. On the other hand, concerning the superfluid density, some phosphorus-substitution compounds have recently revealed nodal features in very low-temperature range.[6,41] This problem is deeply related to the superconducting mechanism while numerical experiments by using the present treatment are ongoing to check the consistency.

Finally, we add a note in terms of the material variety and the gap ratio. According to a recent specific-heat experiment of $Ba(Fe_{0.92}Co_{0.08})_2As_2$,[42] the ratio between the maximum and minimum gaps is around 0.4. This value is a magic number common for optimally doped materials exhibiting the highest T_c, e.g., $Ba_{1-x}K_xFe_2As_2$, $Ba(Fe_{1-x}Co_x)_2As_2$, and $LaFeAs_{1-\delta}O_{1-x}F_x$. This may be not an accidental coincidence because we do not presently know any different compounds. The superconducting mechanism model has to explain the coincidence.

V. CONCLUSION

In conclusion, we examined the validity of $s^{\pm}$-wave scenario for typical iron-based superconductors (122 and 1111 compounds) through the realistic model using the quasiclassical formalism combined with first-principles calculations. Consequently, we found that any anomalous properties observed in the specific heat and the nuclear magnetic relaxation rate are fully reproducible by a set of gap amplitude properly evaluated on each band without any extrinsic assumptions, i.e., a requirement is just gap amplitude of each band together with $s^{\pm}$-wave symmetry.

ACKNOWLEDGMENTS

We acknowledge the fruitful discussions with H. Fukazawa, E. Kaneshita, S. Shamoto, and T. Tohyama. Y.N. acknowledges support by Grant-in-Aid for JSPS (Grant No. 204840).

*nakai.noriyuki@jaea.go.jp

[1] Y. Kamihara, T. Watanabe, M. Hirano, and H. Hosono, J. Am. Chem. Soc. **130**, 3296 (2008).
[2] K. Ishida, Y. Nakai, and H. Hosono, J. Phys. Soc. Jpn. **78**, 062001 (2009).
[3] L. Ding, C. He, J. K. Dong, T. Wu, R. H. Liu, X. H. Chen, and S. Y. Li, Phys. Rev. B **77**, 180510(R) (2008).
[4] G. Mu, H. Luo, Z. Wang, L. Shan, C. Ren, and H.-H. Wen, Phys. Rev. B **79**, 174501 (2009).
[5] Y. Kohama, Y. Kamihara, H. Kawaji, T. Atake, M. Hirano, and H. Hosono, J. Phys. Soc. Jpn. **77**, 094715 (2008).
[6] J. D. Fletcher, A. Serafin, L. Malone, J. G. Analytis, J.-H. Chu, A. S. Erickson, I. R. Fisher, and A. Carrington, Phys. Rev. Lett. **102**, 147001 (2009).
[7] D. V. Evtushinsky, D. S. Inosov, V. B. Zabolotnyy, M. S. Viazovska, R. Khasanov, A. Amato, H.-H. Klauss, H. Luetkens, Ch. Niedermayer, G. L. Sun, V. Hinkov, C. T. Lin, A. Varykhalov, A. Koitzsch, M. Knupfer, B. Buchner, A. A. Kordyuk, and S. V. Borisenko, New J. Phys. **11**, 055069 (2009).
[8] R. S. Gonnelli, D. Daghero, M. Tortello, G. A. Ummarino, V. A. Stepanov, R. K. Kremer, J. S. Kim, N. D. Zhigadlo, and J. Karpinski, Physica C **469**, 512 (2009).
[9] S. L. Bud'ko, N. Ni, and P. C. Canfield, Phys. Rev. B **79**, 220516(R) (2009).
[10] N. Kurita, F. Ronning, Y. Tokiwa, E. D. Bauer, A. Subedi, D. J. Singh, J. D. Thompson, and R. Movshovich, Phys. Rev. Lett. **102**, 147004 (2009).
[11] F. Ronning, E. D. Bauer, T. Park, S.-H. Baek, H. Sakai, and J. D. Thompson, Phys. Rev. B **79**, 134507 (2009).
[12] H. Fukazawa, T. Yamazaki, K. Kondo, Y. Kohori, N. Takeshita, P. M. Shirage, K. Kihou, K. Miyazawa, H. Kito, H. Eisaki, and A. Iyo, J. Phys. Soc. Jpn. **78**, 033704 (2009).
[13] Y. Kobayashi, A. Kawabata, S. C. Lee, T. Moyoshi, and M. Sato, J. Phys. Soc. Jpn. **78**, 073704 (2009).
[14] M. Yashima, H. Nishimura, H. Mukuda, Y. Kitaoka, K. Miyazawa, P. M. Shirage, K. Kiho, H. Kito, H. Eisaki, and A. Iyo, J. Phys. Soc. Jpn. **78**, 103702 (2009).
[15] K. Matano, G. L. Sun, D. L. Sun, C. T. Lin, M. Ichioka, and G.-q. Zheng, EPL **87**, 27012 (2009).
[16] K. Nakayama, T. Sato, P. Richard, Y.-M. Xu, Y. Sekiba, S. Souma, G. F. Chen, J. L. Luo, N. L. Wang, H. Ding, and T. Takahashi, EPL **85**, 67002 (2009).
[17] I. I. Mazin, D. J. Singh, M. D. Johannes, and M. H. Du, Phys. Rev. Lett. **101**, 057003 (2008).
[18] K. Kuroki, H. Usui, S. Onari, R. Arita, and H. Aoki, Phys. Rev. B **79**, 224511 (2009).
[19] The density functional calculation package employed throughout this paper is VASP. G. Kresse and J. Hafner, Phys. Rev. B **47**,

558 (1993); G. Kresse and J. Furthmüller, *ibid.* **54**, 11169 (1996).
[20] T. Kondo, A. F. Santander-Syro, O. Copie, C. Liu, M. E. Tillman, E. D. Mun, J. Schmalian, S. L. Bud'ko, M. A. Tanatar, P. C. Canfield, and A. Kaminski, Phys. Rev. Lett. **101**, 147003 (2008).
[21] D. H. Lu, M. Yi, S.-K. Mo, J. G. Analytis, J.-H. Chu, A. S. Erickson, D. J. Singh, Z. Hussain, T. H. Geballe, I. R. Fisher, and Z.-X. Shen, Physica C **469**, 452 (2009).
[22] K. Hashimoto, T. Shibauchi, T. Kato, K. Ikada, R. Okazaki, H. Shishido, M. Ishikado, H. Kito, A. Iyo, H. Eisaki, S. Shamoto, and Y. Matsuda, Phys. Rev. Lett. **102**, 017002 (2009).
[23] C. Martin, M. E. Tillman, H. Kim, M. A. Tanatar, S. K. Kim, A. Kreyssig, R. T. Gordon, M. D. Vannette, S. Nandi, V. G. Kogan, S. L. Bud'ko, P. C. Canfield, A. I. Goldman, and R. Prozorov, Phys. Rev. Lett. **102**, 247002 (2009).
[24] C. Martin, R. T. Gordon, M. A. Tanatar, H. Kim, N. Ni, S. L. Bud'ko, P. C. Canfield, H. Luo, H. H. Wen, Z. Wang, A. B. Vorontsov, V. G. Kogan, and R. Prozorov, Phys. Rev. B **80**, 020501(R) (2009).
[25] L. Ding, J. K. Dong, S. Y. Zhou, T. Y. Guan, X. Qiu, C. Zhang, L. J. Li, X. Lin, G. H. Cao, Z. A. Xu, and S. Y. Li, New J. Phys. **11**, 093018 (2009).
[26] X. G. Luo, M. A. Tanatar, J.-Ph. Reid, H. Shakeripour, N. Doiron-Leyraud, N. Ni, S. L. Bud'ko, P. C. Canfield, H. Luo, Z. Wang, H.-H. Wen, R. Prozorov, and L. Taillefer, Phys. Rev. B **80**, 140503(R) (2009).
[27] M. A. Tanatar, J. P. Reid, H. Shakeripour, X. G. Luo, N. Doiron-Leyraud, N. Ni, S. L. Bud'ko, P. C. Canfield, R. Prozorov, and L. Taillefer, Phys. Rev. Lett. **104**, 067002 (2010).
[28] B. Mitrović and K. V. Samokhin, Phys. Rev. B **74**, 144510 (2006).
[29] Y. Bang, H.-Y. Choi, and H. Won, Phys. Rev. B **79**, 054529 (2009).
[30] Y. Nagai, N. Hayashi, N. Nakai, H. Nakamura, M. Okumura, and M. Machida, New J. Phys. **10**, 103026 (2008).
[31] G. Eilenberger, Z. Phys. **214**, 195 (1968).
[32] N. Kopnin, *Theory of Nonequilibrium Superconductivity* (Oxford University Press, New York, 2005), Chap. 5.
[33] H. Suhl, B. T. Matthias, and L. R. Walker, Phys. Rev. Lett. **3**, 552 (1959).
[34] K. Watanabe and T. Kita, J. Phys. Soc. Jpn. **73**, 2239 (2004).
[35] V. G. Kogan, C. Martin, and R. Prozorov, Phys. Rev. B **80**, 014507 (2009).
[36] $\omega_c = 2000 T_c$ is used in calculating pair potentials and free energy. To obtain the second derivative of F_{sn} precisely by numerical derivative, we need such a large ω_c.
[37] M. Rotter, M. Tegel, D. Johrendt, I. Schellenberg, W. Hermes, and R. Pöttgen, Phys. Rev. B **78**, 020503(R) (2008).
[38] C. de la Cruz, Q. Huang, J. W. Lynn, J. Li, W. Ratcliff II, J. L. Zarestky, H. A. Mook, G. F. Chen, J. L. Luo, N. L. Wang, and P. Dai, Nature (London) **453**, 899 (2008).
[39] M. Sato, Y. Kobayashi, S. C. Lee, H. Takahashi, E. Satomi, and Y. Miura, J. Phys. Soc. Jpn. **79**, 014710 (2010).
[40] F. Hammerath, S.-L. Drechsler, H.-J. Grafe, G. Lang, G. Fuchs, G. Behr, I. Eremin, M. M. Korshunov, and B. Büchner, Phys. Rev. B **81**, 140504(R) (2010).
[41] K. Hashimoto, M. Yamashita, S. Kasahara, Y. Senshu, N. Nakata, S. Tonegawa, K. Ikada, A. Serafin, A. Carrington, T. Terashima, H. Ikeda, T. Shibauchi, and Y. Matsuda, Phys. Rev. B **81**, 220501(R) (2010).
[42] K. Gofryk, A. S. Sefat, E. D. Bauer, M. A. McGuire, B. C. Sales, D. Mandrus, J. D. Thompson, and F. Ronning, New J. Phys. **12**, 023006 (2010).